Cell Transplantation, Vol. 26, pp. 243–257, 2017

0963-6897/17 $90.00 + .00
DOI: https://doi.org/10.3727/096368916X693031
E-ISSN 1555-3892
www.cognizantcommunication.com

Secondary Release of Exosomes From Astrocytes Contributes to the Increase in Neural Plasticity and Improvement of Functional Recovery After Stroke in Rats Treated With Exosomes Harvested From MicroRNA 133b-Overexpressing Multipotent Mesenchymal Stromal Cells

Hongqi Xin,* Fengjie Wang,* Yanfeng Li,* Qing-e Lu,* Wing Lee Cheung,† Yi Zhang,* Zheng Gang Zhang,* and Michael Chopp*‡

*Department of Neurology, Henry Ford Hospital, Detroit, MI, USA
†Department of Emergency Medicine, Henry Ford Hospital, Detroit, MI, USA
‡Department of Physics, Oakland University, Rochester, MI, USA

We previously demonstrated that multipotent mesenchymal stromal cells (MSCs) that overexpress microRNA 133b (miR-133b) significantly improve functional recovery in rats subjected to middle cerebral artery occlusion (MCAO) compared with naive MSCs and that exosomes generated from naive MSCs mediate the therapeutic benefits of MSC therapy for stroke. Here we investigated whether exosomes isolated from miR-133b-overexpressing MSCs (Ex-miR-133b$^+$) exert amplified therapeutic effects. Rats subjected to 2 h of MCAO were intra-arterially injected with Ex-miR-133b$^+$, exosomes from MSCs infected by blank vector (Ex-Con), or phosphate-buffered saline (PBS) and were sacrificed 28 days after MCAO. Compared with the PBS treatment, both exosome treatment groups exhibited significant improvement of functional recovery. Ex-miR-133b$^+$ treatment significantly increased functional improvement and neurite remodeling/brain plasticity in the ischemic boundary area compared with the Ex-Con treatment. Treatment with Ex-miR-133b$^+$ also significantly increased brain exosome content compared with Ex-Con treatment. To elucidate mechanisms underlying the enhanced therapeutic effects of Ex-miR-133b$^+$, astrocytes cultured under oxygen- and glucose-deprived (OGD) conditions were incubated with exosomes harvested from naive MSCs (Ex-Naive), miR-133b downregulated MSCs (Ex-miR-133b$^-$), and Ex-miR-133b$^+$. Compared with the Ex-Naive treatment, Ex-miR-133b$^+$ significantly increased exosomes released by OGD astrocytes, whereas Ex-miR-133b$^-$ significantly decreased the release. Also, exosomes harvested from OGD astrocytes treated with Ex-miR-133b$^+$ significantly increased neurite branching and elongation of cultured cortical embryonic rat neurons compared with the exosomes from OGD astrocytes subjected to Ex-Con. Our data suggest that exosomes harvested from miR-133b-overexpressing MSCs improve neural plasticity and functional recovery after stroke with a contribution from a stimulated secondary release of neurite-promoting exosomes from astrocytes.

Key words: MicroRNA 133b (miR-133b); Exosome; Multipotent mesenchymal stromal cell (MSCs); Neural plasticity; Astrocyte; Stroke; Functional recovery

INTRODUCTION

Multipotent mesenchymal stromal cells (MSCs) enhance functional recovery in experimental stroke models by amplifying neurogenesis, angiogenesis, and neural plasticity[1–5]. Our prior in vitro and in vivo studies indicated that the therapeutic benefits of MSC-based therapies are mediated by exosome-enriched extracellular particles that transfer microRNAs (miRNAs) from MSCs to neural cells[6–10]. This exosome transfer of miRNAs evokes neurite remodeling and brain plasticity and subsequently benefits functional recovery[6,8]. Treatment of rats subjected to middle cerebral artery occlusion (MCAO) with MSCs overexpressing microRNA 133b (miR-133b) augments neurite remodeling and brain plasticity and subsequently improves functional recovery[6]. Whether treatment of stroke with cell-free exosomes enriched with miR-133b affects brain plasticity and neurological recovery has not been investigated.

Exosomal release is regulated by specific physiological and pathological conditions[11–13] and by multivesicular body (MVB) fusion with the plasma membrane. Factors

Received June 13, 2016; final acceptance July 17, 2016. Online prepub date: September 26, 2016.
Address correspondence to Hongqi Xin, Ph.D., Department of Neurology, Henry Ford Hospital, 2799 West Grand Boulevard, Detroit, MI 48202, USA. Tel: 313-916-7271; Fax: 313-916-1318; E-mail: hongqi@neuro.hfh.edu, hxin1@hfhs.org

that impact MVB fusion affect exosome secretion, for example, intracellular calcium[14–16], K^+-induced depolarization[15], and glutaminergic activity[17]. Extracellular exosomes may also impact the exosomes released by the recipient cells. An in vitro study has shown that exosomes from normal human mammary epithelial cells inhibit exosome secretion from breast cancer cells by means of negative feedback control after intake of the epithelial cell exosomes by breast cancer cells[18].

Here we intra-arterially (IA) administered miR-133b-enriched exosomes derived from MSCs to rats subjected to MCAO and investigated whether these exosomes exert amplified therapeutic effects compared with the control MSC exosomes. We demonstrated that exosomes tailored with enriched miR-133b from MSCs enhance neurological recovery and plasticity poststroke compared with the control MSC exosomes. We further demonstrated, for the first time, using in vivo and in vitro approaches, that miR-133b-enriched exosomes amplify neurite outgrowth poststroke by stimulating secondary release of astrocytic exosomes.

MATERIALS AND METHODS

All experimental procedures were carried out in accordance with the National Institutes of Health (NIH) Guide for the Care and Use of Laboratory Animals and were approved by the Institutional Animal Care and Use Committee (IACUC) of the Henry Ford Health System. All exosome-enriched extracellular vesicles (EVs) were collected using multistep ultracentrifugation, and their sizes were verified by transmission electron microscopy as well as Western blot detection of common exosomal proteins, CD63[19,20] and CD81[21,22]. For simplification, in the present study, we refer to these EVs as exosomes.

Production for miR-133b Knockin or Knockdown MSC Exosomes

MSCs (three to four passages (P3~4)] were dissociated from Wistar rat bone marrow, cultured, and then infected with lentivirus, as previously described[6,23–25]. The lentivirus was constructed with the vectors of LentimiRa-GFP-hsa-miR-133b Vector (mh10170; pre-miR-133b was inserted for miR-133b knockin, Lenti-miR-133b$^+$; Applied Biological Materials Inc., Richmond, Canada), pLenti-III-miR-GFP Control Vector (m001; vector for miR-133b knockin control, Lenti-miR-CON$^+$; Applied Biological Materials Inc.), miRZip-133b anti-miR-133b miRNA construct (MZIP133b-PA-1; miR-133b inhibitor inserted for miR-133b knockdown, Lenti-miR-133b$^-$; System Biosciences, LLC, Palo Alto, CA, USA), and pGreenPuro Scramble Hairpin Control Construct (MZIP000-PA-1; vector for miR-133b knockdown control, Lenti-miR-CON$^-$; System Biosciences, Inc.), respectively, according to the manufacturer's suggested protocol. MSCs were infected with lentivirus when they achieved 80%–90% confluence and were selected by puromycin for constant gene expression. Correspondingly, the MSCs generated are referred to as miR-133b$^+$MSCs,miR-CON$^+$MSCs,miR-133b$^-$MSCs,and miR-CON$^-$MSCs, respectively. For the harvesting of exosomes, we replaced conventional culture medium with an exosome-depleted fetal bovine serum (FBS; EXO-FBS-250A-1; System Biosciences, Inc.) medium when the cells reached 60%–80% confluence. After an additional 24 h of culturing, the media were then collected and centrifuged at $3{,}000\times g$ for 30 min to remove the dead cells and large cell apoptotic bodies; then the upper media were stored in a −80°C freezer for exosome isolation.

MCAO Model, Exosome Treatment, and Behavioral Tests

In our previous in vivo stroke studies, we administered exosomes intravenously[7]. In addition, we have shown that direct application of MSC exosomes on cultured cortical neurons induces neurite outgrowth via transfer of miR-133b[8]. In the current study, in order to reduce the potential liver and lung sequestration of exosomes[26,27] and to optimize the MSC exosome localization with neural parenchymal cells, we administered the exosomes using an IA approach.

Adult male Wistar rats (weighing 270–300 g) were purchased from Charles River Laboratories (Wilmington, MA, USA) and were subjected to 2 h of MCAO using a method of intraluminal vascular occlusion as modified in our laboratory[28,29]. Briefly, rats were anesthetized with 3.5% isoflurane for induction and maintained by spontaneously respired 1.0% isoflurane in a 2:1 N_2O/O_2 mixture using a face mask. The rectal temperature was kept at 37 ± 1°C throughout the surgical procedure using a feedback-regulated water-heating system. MCAO was induced by advancing a 4-0 surgical nylon suture, with its tip rounded by heating near a flame, from the external carotid artery into the lumen of the internal carotid artery (ICA) to block the origin of the right middle cerebral artery (MCA). After 2 h of MCAO, animals were reanesthetized with isoflurane, and reperfusion was performed by withdrawal of the suture until the tip cleared the lumen of the external carotid artery. The procedure provides a focal infarct in the unilateral striatum and cortex[28,30].

Twenty-four hours after induction of stroke, rats were randomly administered exosomes (3×10^{11} particles, comparable to 100 μg of total exosome protein, per rat) harvested from miR-CON$^+$MSCs (Ex-Con) or from miR-133b$^+$MSCs (Ex-miR-133b$^+$) dissolved into 0.5 ml of phosphate-buffered saline (PBS; Thermo Fisher Scientific Inc., Grand Island, NY, USA) or 0.5 ml of PBS as vehicle control ($n=6$/group).

For evaluation of functional recovery, a foot fault test[31] and a modified neurologic severity score (mNSS) test[32]

were performed prior to MCAO and 1, 3, 7, 14, 21, and 28 days after MCAO by an investigator blinded to the treatments. All rats were sacrificed 28 days after MCAO. Rat brains were snap frozen in liquid nitrogen, and the frozen coronal sections were cut (40-μm thickness for molecular studies, e.g., Western blot and exosome extraction; 8-μm thickness for immunohistochemical staining) and stored in −80°C for subsequent analysis.

Exosome Isolation and Quantification

Exosome isolation from the cell cultured media was performed at 4°C via multistep centrifugation, as previously described[7,8,33]. Briefly, the stocked cultured cell media were thawed and followed by vortex mixing for 1 min before centrifugation, and then centrifuged at 10,000×*g* for 30 min to remove large debris. The supernatants were filtered through a 0.22-μm filter (SLMP025SS; EMD Millipore Corporation, Billerica, MA, USA) to remove small cell debris, and the resulting media were further centrifuged at 100,000×*g* for 2 h. By this step, the pellets primarily contained exosomes[33]. The final exosome pellets harvested from 1×10^7 cells were identified, as previously described[8], and resuspended in 30 to 50 μl of PBS and stored at −80°C for further use.

Exosomes in the ischemic boundary zone (IBZ) were extracted by following a previously described protocol with modification[34]. Briefly, the IBZ tissues from frozen rat brain sections were collected and digested with 20 U/ml papain (LS 03126; Worthington Biochemical Corp., Lakewood, NJ, USA) in Hibernate E solution (20 μl/mg brain tissue; Life Technologies Corporation, Grand Island, NY, USA) for 15 min at 37°C. The brain tissue was gently homogenized in two volumes of cold Hibernate E solution. The brain homogenate was sequentially filtered through a Falcon™ 40-μm mesh filter (Catalog No. 08-771-1; Thermo Fisher Scientific, Hampton, NH, USA). Exosomes were isolated from the filtrate, as previously described[15]. Briefly, the filtrate was sequentially centrifuged at 300×*g* for 10 min at 4°C, 2,000×*g* for 10 min at 4°C, 10,000×*g* for 30 min at 4°C and filtered through 0.2-μm syringe filters to discard cells, membranes, and debris. The supernatant was centrifuged at 100,000×*g* for 2 h at 4°C to pellet exosomes. The exosome pellet was resuspended in cold PBS, and the exosome solution was centrifuged at 100,000×*g* for 2 h at 4°C.

Exosomes were identified by the marker protein CD63[19,20] or CD81[21,22] using Western blot, as well as by transmission electron microscopy (TEM) to verify the exosome size[35,36]. We quantitated the exosomes by measuring the total protein concentration, assessed by the micro bicinchoninic acid (BCA) protocol (Pierce, Rockford, IL, USA)[37] and by a qNano particle analyzer (Izon Science Ltd., Cambridge, MA, USA) for exosome particle number.

In Vitro Primary Astrocyte Culture and Treatments

Extracts from cortices of embryonic day 18 Wistar rats (either sex; Charles River Laboratories) were dissociated into a cell suspension using mechanical digestion. After digestion, cells were plated in 75-cm^2 tissue culture flasks at a concentration of 1.5×10^7 cells in Dulbecco's modified Eagle's medium (DMEM; Catalog No. 11995-065; Thermo Fisher Scientific) containing 20% FBS. The flasks were incubated at 37°C in a moist 5% CO_2, 95% air atmosphere for 48–72 h before moving. The medium was changed every 48–72 h. After incubating the primary cultures for 7–9 days, the flasks were placed on a shaker platform in a horizontal position with the medium covering the cells and were shaken at 350 rpm for 6 h at 35°C to separate oligodendrocytes from the astrocytes. Medium was changed and flasks were placed on the shaker for an additional 18 h. Afterward, medium was again changed and shook for an additional 24 h. When confluent, cells were passed and used for MSC exosome treatment. To mimic the in vivo ischemic condition, an in vitro oxygen- and glucose-deprived (OGD) culture system on astrocytes was employed, as previously described[38]. Primary cultured astrocytes were washed twice with PBS before MSC exosome treatment, and then the media containing exosomes (3×10^{10} particles/ml) or media alone were added to the cultured cells.

Neurite Outgrowth Assay

Primary cultures of cortical neurons were harvested from embryonic day 18 Wistar rats, as previously described[39]: Pregnant rats purchased from Charles River Laboratories were euthanized under deep pentobarbital anesthesia. Embryos were removed, and the cerebral cortex was dissected out, washed in Hank's balanced salt solution (HBSS; Gibco, Grand Island, NY, USA), and dissociated by a combination of 0.125% trypsin digestion for 15 min, then mechanically triturated 20 times. The triturated cells were passed through a 40-μm cell strainer and counted to obtain a concentration of 3×10^7 cells/ml.

For the neurite outgrowth assay, the neurons were then plated overnight onto a poly(D-lysine)-coated 24-well plate at a density of 5,000 cells per well in DMEM containing 5% FBS and antibiotics. After 24 h, cells were washed three times with PBS and treated with various astrocytic-derived exosomes dissolved at a concentration of 3×10^{10} particles/ml into the serum-free neurobasal medium (Gibco) supplemented with 2% B-27 (Gibco), 500 μM L-glutamine, and antibiotics (Catalog No. G6784; Sigma-Aldrich, St. Louis, MO, USA). After 3 days, neurons were washed and fixed with 4% paraformaldehyde (PFA) and immunofluorescence staining for β-III-tubulin (TuJ1) for neurite outgrowth analysis, as previously described[39]. Briefly, to analyze neurite outgrowth, $TuJ1^+$ cells were digitized using a 20× objective (Carl Zeiss Microscopy, LLC, Thornwood, NY, USA) via the Micro

Computer Imaging Device (MCID) analysis system (Imaging Research, St. Catharines, Canada). Neurite outgrowth was quantified using a software program developed in our laboratory that includes measurements of the number and length of branches[40]. At least 50 TuJ1$^+$ cells, distributed in nine random fields per well, and triple wells per group were measured, and three independent experiments were performed. All measurements were performed by experimenters blinded to each culture condition.

miRNA Assay

For the measurement of miR-133b in exosomes from cultured cells, samples were lysed in QIAzol reagents, and the total RNA was isolated using the miRNeasy Mini Kit (Qiagen, Valencia, CA, USA). By real-time polymerase chain reaction (RT-PCR), we detected the miR-133b level. Briefly, miRNAs were reverse transcribed with the miRNA Reverse Transcription Kit (Applied Biosystems, Foster City, CA, USA), and PCR amplification was performed with the TaqMan miRNA Assay Kit (which is specific for mature miRNA sequences; Applied Biosystems) according to the manufacturer's protocols, with U6 snRNA as an internal control.

Histopathology and Immunohistochemistry

To determine neurite remodeling in the IBZ, adjacent frozen coronal sections of rat brains were used for staining the following markers, and positive staining within the IBZ was measured under light microscopy. Bielschowsky silver (silver nitrate; stains neuronal processes[41]; Sigma-Aldrich) combined with Luxol fast blue (stains myelin sheath[42]; Sigma-Aldrich) histochemistry staining as well as immunostaining with antibodies against the phosphorylated epitope of neurofilament heavy polypeptide (NF-H), clone SMI 31 (SMI 31; reacts broadly with thick and thin axons and some dendrites[43]), and synaptophysin (a marker for synapses, since synaptophysin is ubiquitously present at the synapses[44]) were employed, respectively. Briefly, for immunostaining, adjacent frozen brain sections were incubated with the primary antibodies against SMI 31 (1:500; ab82259; Abcam, Cambridge, MA, USA), synaptophysin (1:100; MAB5258; Chemicon, Billerica, MA, USA), and BrdU (1:100; Roche Diagnostics Corporation, Indianapolis, IN, USA), followed with corresponding horseradish peroxidase (HRP)-conjugated secondary antibodies (Abcam) and 3,3′-diaminobenzidine (DAB; Sigma-Aldrich) developing, respectively. Positive staining within nine areas (four from the cortex, four from the striatum, and one from the corpus callosum) selected along the IBZ in these groups were digitized under a 40× objective (BX40; Olympus Optical, Waltham, MA, USA) using a 3-CCD color video camera (DXC-970MD; Sony, Teaneck, NJ, USA) interfaced with the MCID™ software[45]. For the analysis of neurite remodeling, based on evaluation of an average of three histology slides (8-μm thick, interval of every 10th slide) from the standard block of each animal, the percentage of positive staining area to the whole area of each image taken within the IBZ was analyzed using the MCID™ software.

To detect astrocytic expression of Rab9 effector protein with kelch motifs (RABEPK) in the IBZ, double immunofluorescence staining was employed to identify the cellular colocalization of RABEPK (1:100; sc-107078; Santa Cruz Biotechnology, Dallas, TX, USA) with glial fibrillary acidic protein (GFAP; a marker of reactive astrocyte; 1:10,000; Z0334; Dako, Carpinteria, CA, USA), followed by their corresponding second antibody staining [fluorescein isothiocyanate (FITC) labeled for RABEPK and Cy3 labeled for GFAP].

Statistical Analysis

Data are summarized and presented using mean ± standard error (SE). Post hoc tests were used for subgroup analysis following analysis of variance (ANOVA). The Global test using the generalized estimating equation (GEE) was employed to evaluate the MSC exosome treatment effects influenced by miR-133b enrichment on functional recovery[46,47]. Repeated-measures analysis was used to evaluate data with repeated measurements over time (e.g., functional tests) or histological evaluation on multiple regions per subject. Analysis began testing for the factor interaction, followed by testing the main factor effect if no interaction was detected at the 0.05 level, and/or a subgroup analysis was performed if the interaction or main effect was detected at the 0.05 level[48]. All statistical analyses were conducted using the SAS software (version 9.2; SAS Institute, Cary, NC, USA).

RESULTS

miR-133b Level Modified by Lentivirus Introduction of Pre-miR-133b and miR-133b Inhibitors

Quantitative RT-PCR analysis showed that mature miR-133b levels in the MSCs infected by lentivirus carrying pre-miR-133b were increased and, concomitantly, miR-133b levels in exosomes harvested from these MSCs significantly increased (Table 1). Correspondingly, the miR-133b levels in MSCs and harvested exosomes were significantly decreased by introducing an miR-133b inhibitor into MSCs (Table 1). There was no statistical difference in miR-133b levels among naive MSCs and MSCs infected by blank vector controls (miR-CON$^+$MSCs and miR-CON$^-$MSCs) as well as in their corresponding exosomes (Table 1).

miR-133b-Enriched Exosomes Improve Neurological Outcome After MCAO

Tailored exosomes enriched with miR-133b as well as the exosomes harvested from blank vector control

Table 1. Relative miR-133b Level in the Various Lentivirus-Infected MSCs and Their Corresponding Exosomes

Groups	In Cells (Relative Fold)	In Exosomes (Relative Fold)
Naive MSCs	1.0	1.0
miR-CON$^+$MSCs	1.01 ± 0.21	0.98 ± 0.23
miR-133b$^+$MSCs	432.65 ± 125.01*	8.83 ± 2.31*
miR-CON$^-$MSCs	1.02 ± 0.13	1.01 ± 0.34
miR-133b$^-$MSCs	0.23 ± 0.19†	0.45 ± 0.11†

*$p < 0.01$ compared with the miR-CON$^+$MSCs; †$p < 0.05$ compared with the miR-CON$^-$MSCs.

MSCs administered IA to rats subjected to 2 h of transient MCAO significantly reduced neurological deficits compared with the PBS-treated rats. Foot fault and mNSS tests were performed to assess the sensorimotor function. All rats exhibited severe sensorimotor deficit at postoperative day 1, followed by gradual improvement within the 4-week experimental course. Compared with the PBS treatment, both exosome treatment groups exhibited significant improvement of functional recovery in the foot fault test (Fig. 1A) and mNSS (Fig. 1B); however, significant improvement was detected at 7 and 14 days after MCAO in the Ex-miR-133b$^+$ and the Ex-Con treatment groups, respectively. Compared with the Ex-Con, the Ex-miR-133b$^+$ treatment significantly increased functional improvement ($p < 0.05$ after day 21, respectively) (Fig. 1A and B).

miR-133b-Enriched Exosomes Enhance Neurite Remodeling in the IBZ

Stroke evokes partial damage and disorganization to axon–myelin bundles in the IBZ[49]. Double staining for Bielschowsky silver and Luxol fast blue was employed to identify axons and myelin in the white matter in the brain, respectively. Axonal density along the IBZ was significantly increased by the exosome treatment compared with the PBS control 28 days after MCAO, and Ex-miR-133b$^+$ further increased the axonal density compared with the Ex-Con ($p < 0.05$, respectively) (Fig. 2, row A).

The phosphorylation of the neurofilament (NF) is considered an important determinant of filament caliber, plasticity, and stability[50]. Immunocytochemically purified anti-NF-H phosphorylated antibody (clone SMI 31) reacts broadly with thick and thin axons and some dendrites such as basket cell dendrites, but not Purkinje cell

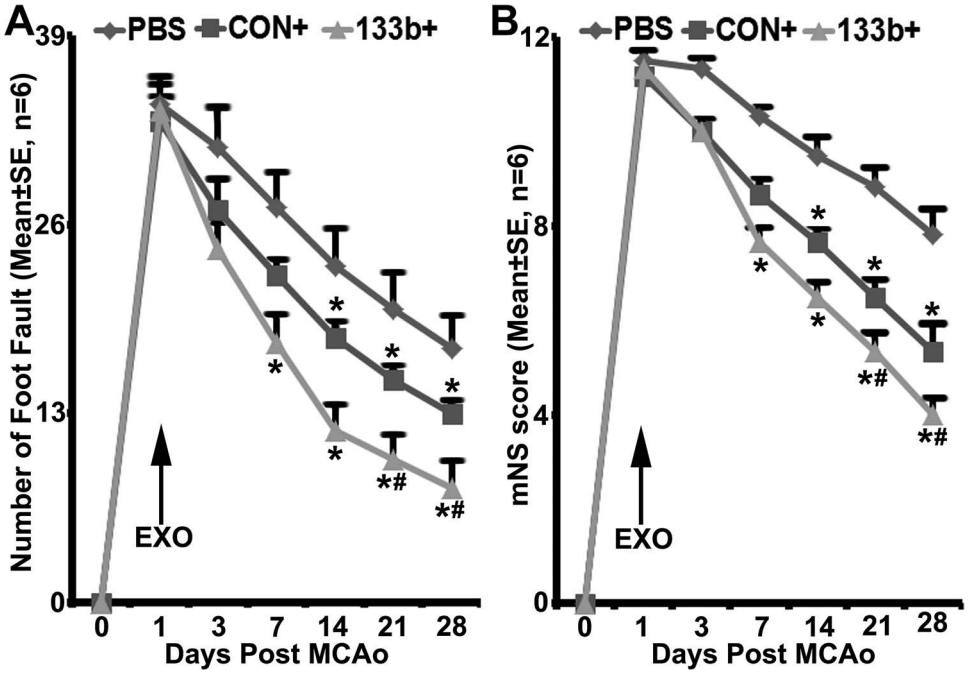

Figure 1. MicroRNA 133b (miR-133b)-enriched exosome treatment enhances neurological outcome improvement. Foot fault test (A) and modified neurologic severity score (mNSS) (B) data show that compared with the phosphate-buffered saline (PBS) treatment, both multipotent mesenchymal stromal cell (MSC) exosome treatment groups exhibited significant improvement of functional recovery ($p < 0.05$ after day 14, respectively). Compared with the MSCs infected with blank vector (Ex-Con), exosomes isolated from miR-133b-overexpressing MSCs (Ex-miR-133b$^+$) significantly increased functional improvement ($p < 0.05$ after day 21, respectively). PBS, middle cerebral artery occlusion (MCAO) rats treated with PBS; CON$^+$, MCAO rats treated with Ex-Con; 133b$^+$, MCAO rats treated with Ex-miR-133b$^+$; EXO, exosomes given. *$p < 0.05$, compared to PBS; #$p < 0.05$ compared to CON$^+$, respectively. Mean ± standard error (SE), $n = 6$/group.

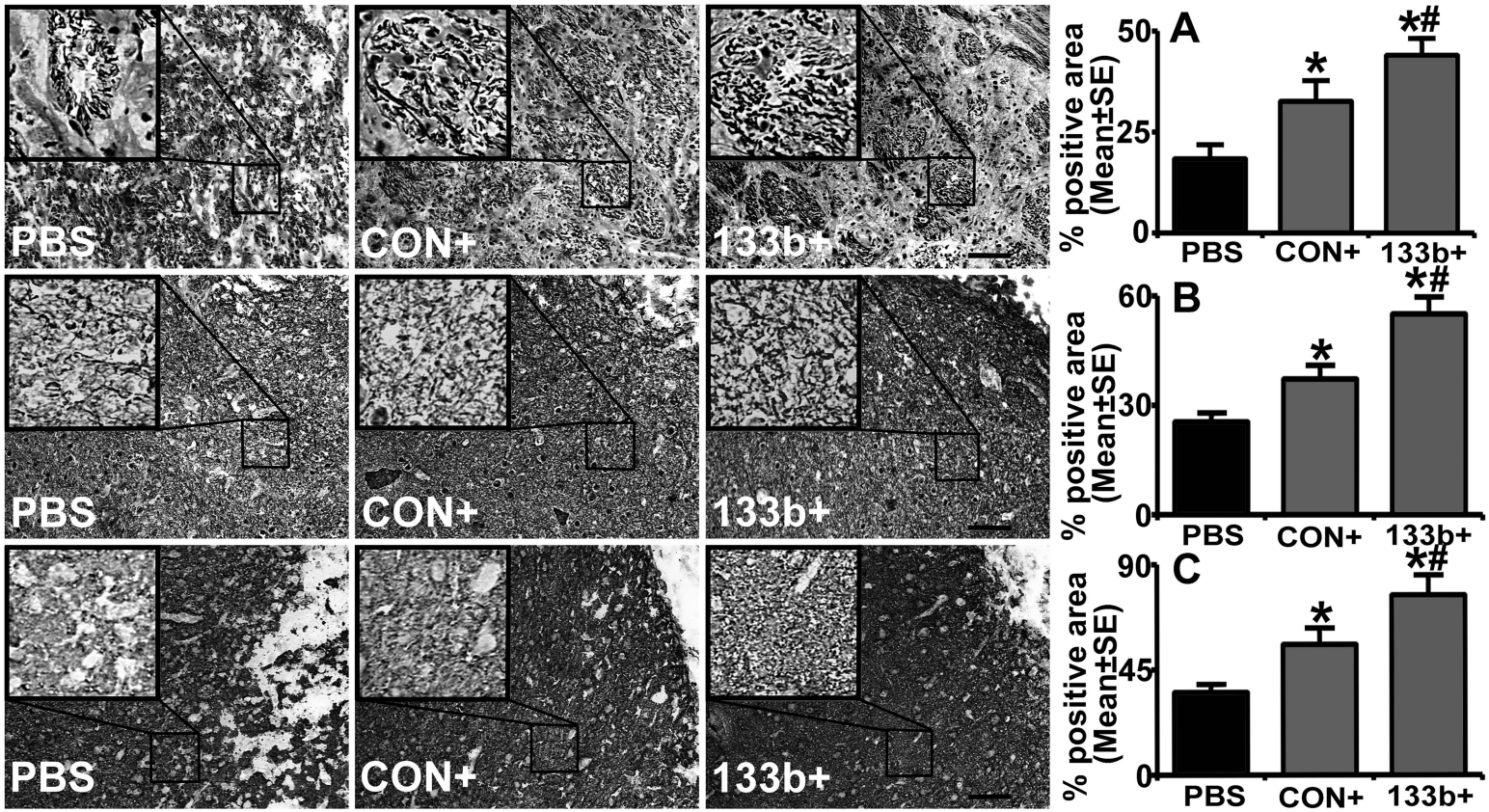

Figure 2. MicroRNA 133b (miR-133b)-enriched exosomes further increase neurite remodeling and synaptic plasticity in the ischemic boundary zone (IBZ) compared to control multipotent mesenchymal stromal cell (MSC) exosomes. Bielschowsky silver and Luxol fast blue double staining (A row), SMI 31 immunostaining (B row), and synaptophysin immunostaining (C row) show that based on the increase of neurite remodeling and synaptic plasticity in the IBZ by the MSCs infected with blank vector (Ex-Con) treatment, the exosomes isolated from miR-133b-overexpressing MSC (Ex-miR-133b$^+$) treatment further increased neurite remodeling and synaptic plasticity in the IBZ. PBS, middle cerebral artery occlusion (MCAO) rats treated with phosphate-buffered saline (PBS); CON$^+$, MCAO rats treated with Ex-Con; 133b$^+$, MCAO rats treated with Ex-miR-133b$^+$. *$p<0.05$, compared to PBS; #$p<0.05$ compared to CON$^+$, respectively. Mean ± standard error (SE), $n=6$/group. Scale bars: 100 μm.

dendrites, and immunohistochemistry staining with this antibody reveals the accumulation of phosphorylated NF-H (p-NFH) in axons and dendrites in the peri-infarct region after stroke[51]. Our data showed that the exosome treatment significantly increased the p-NFH immunoreactive area in the IBZ compared with the PBS control 28 days after MCAO, and similarly, Ex-miR-133b$^+$ further increased the p-NFH immunoreactivity compared with the Ex-Con ($p<0.05$, respectively) (Fig. 2, row B).

Immunostaining data also showed that compared with the PBS control, the MSC exosome treatment significantly increased synaptophysin, a presynaptic vesicle protein that identifies synaptic plasticity and synaptogenesis[52] in the IBZ 28 days after MCAO, while Ex-miR-133b$^+$ further increased the synaptophysin immunoreactivity compared with the Ex-Con ($p<0.05$, respectively) (Fig. 2, row C).

miR-133b-Enriched Exosomes Increase Exosomes in Ischemic Brain

Cellular release of vesicles containing functional components (e.g., RNAs and proteins) that are taken up and incorporated into the target recipient cell has emerged as a regulatory mechanism for coordination of nervous system function[53–55]. Exosomes released by astrocytes and other glial cells in the central nervous system (CNS) likely modulate neuron–glial–vascular communication and support neural plasticity[33,56–58]. We therefore measured the amount of exosomes present in the IBZ. Our data show that the Ex-miR-133b$^+$ treatment significantly increased the presence of exosomes in brain IBZ compared with the Ex-Con treatment ($p<0.05$) (Fig. 3C) and the PBS treatment.

miR-133b-Enriched Exosomes Increase the Release of Exosomes From Cultured Primary Astrocytes

Since astrocytes are the most abundant cells in the nervous system and play an active role in brain recovery[59–61], and OGD culture has been used as an in vitro model to mimic the in vivo ischemic condition[62–64], we employed OGD-cultured astrocytes to elucidate mechanisms underlying the enhanced therapeutic effects of Ex-miR-133b$^+$ on rats subjected to MCAO. First, we investigated the effects of Ex-miR-133b$^+$ on astrocyte exosomal release. OGD astrocytes were incubated with Ex-Naive, Ex-miR-133b$^-$, and Ex-miR-133b$^+$, as well as exosomes from miR-CON$^+$MSCs and miR-CON$^-$MSCs, and the release of exosomes from astrocytes was quantified. Our data showed that astrocytes subjected to OGD increased exosomal release, while MSC exosomes further significantly increased exosomes released by OGD astrocytes. There was no statistically significant difference of exosomes released by OGD astrocytes among the naive MSC exosomes and the two control MSC exosome treatments (Fig. 4A). However, compared with the Ex-Naive

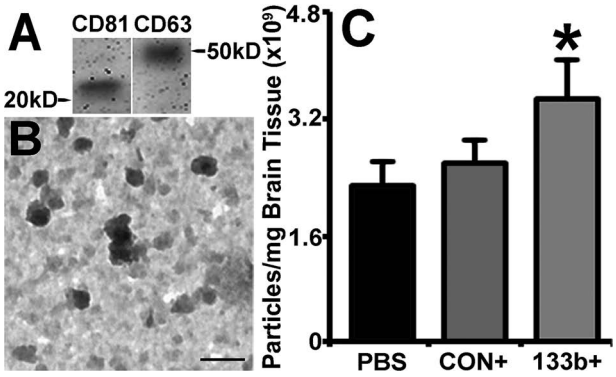

Figure 3. MicroRNA 133b (miR-133b)-enriched exosomes increased exosomes in brain ischemic boundary zone (IBZ). Western blot shows that the common exosomal proteins CD63 and CD81 are present in the exosome extraction from the IBZ (A). The transmission electron microscopic (TEM) images show the morphology of exosomes presented in the brain extracellular (B), within a size range of 30–100 nm. qNano quantification data show that compared to the multipotent mesenchymal stromal cells (MSCs) infected with blank vector (Ex-Con) treatment and phosphate-buffered saline (PBS) control, the extracellular exosomes present in the IBZ significantly increased after miR-133b-overexpressing MSC (Ex-miR-133b$^+$) treatment (C). PBS, middle cerebral artery occlusion (MCAO) rats treated with PBS; CON$^+$, MCAO rats treated with Ex-Con; 133b$^+$, MCAO rats treated with Ex-miR-133b$^+$. *$p<0.05$, compared to Ex-Con. Mean ± standard error (SE), $n=6$/group. Scale bar: 100 nm.

treatment, Ex-miR-133b$^+$ significantly increased exosomes released by OGD astrocytes ($p<0.05$) (Fig. 4A), whereas incubation of OGD astrocytes with Ex-miR-133b$^-$ significantly decreased the OGD astrocytes to release exosomes ($p<0.05$) (Fig. 4B). In a complementary experiment, we also investigated the effect of overexpression of miR-133b on MSCs to release exosomes. Infection of MSCs with the blank vector controls did not significantly affect MSCs to release exosomes compared to naive MSCs. However, overexpression or inhibition of miR-133b significantly increased or decreased, respectively, MSC release of exosomes compared to naive MSCs ($p<0.05$) (Fig. 4B).

Exosomes Harvested From OGD Astrocytes Treated With Ex-miR-133b$^+$ Increase Neurite Outgrowth

By employing the primary cortical neuronal neurite outgrowth assay, we tested the effects of OGD astrocyte exosomes on neurite branching and elongation of the neurons. Our data show that exosomes harvested from OGD astrocytes significantly increased the neurite branch number and total neurite length per neuron compared with the non-exosome-treated neurons. Compared to exosomes from astrocytes subjected to OGD only, exosomes harvested from OGD astrocytes pretreated by Ex-Con and Ex-miR-133b$^+$ substantially increased the neurite branch number and total neurite length of

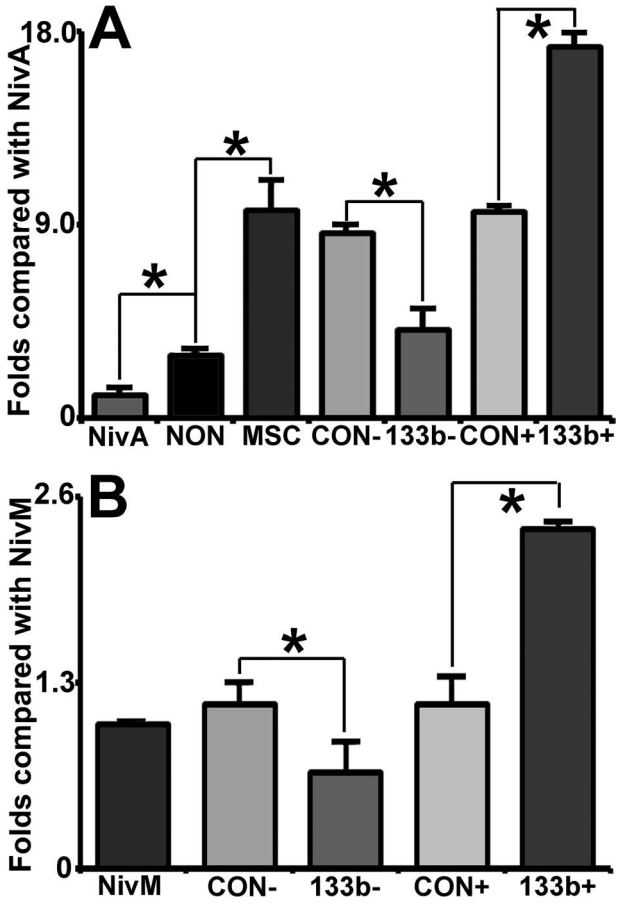

Figure 4. MicroRNA 133b (miR-133b)-enriched exosomes enhance the release of exosomes from primary cultured oxygen- and glucose-deprived (OGD) astrocytes. MSC exosomes significantly increased the exosomes released by OGD astrocytes, and there was no obvious difference on the release from OGD astrocytes, after treatment with harvested from naive MSCs (Ex-Naive) and two control exosomes (A). Compared with the exosome Ex-Naive treatment, exosomes released by OGD astrocytes treated with miR-133b-overexpressing MSCs (Ex-miR-133b$^+$) were significantly increased (A) and significantly decreased (B) by treatment with Ex-miR-133b$^-$, respectively. Correlated with the miR-133b levels in the multipotent mesenchymal stromal cells (MSCs) (Table 1), the number of exosomes released by MSCs has no difference between naive MSCs and the two control MSCs (miR-CON$^+$MSCs and miR-CON$^-$MSCs), but the exosomal release was significantly increased from the miR-133b$^+$MSCs and decreased from the miR-133b$^-$MSCs, compared with that from naive MSCs (B). NivM, naive MSCs; NivA, naive astrocytes; NON, nontreated OGD astrocytes; MSC, OGD astrocytes treated with naive MSC exosomes; CON$^-$, miR-CON$^-$MSC or OGD astrocytes treated with miR-CON$^-$MSC exosomes; 133b$^-$, miR-133b$^-$MSC or OGD astrocytes treated with miR-133b$^-$MSC exosomes; CON$^+$, miR-CON$^+$MSC or OGD astrocytes treated with miR-CON$^+$MSC exosomes; 133b$^+$, miR-133b$^+$MSC or OGD astrocytes treated with miR-133b$^+$MSC exosomes. *$p<0.05$, mean±SD, $n=3$/group.

primary cultured cortical neurons, while exosomes from OGD astrocytes treated by Ex-miR-133b$^+$ employed to treat primary cortical neurons had more robust effects on neurite outgrowth compared with the exosomes from OGD astrocytes with Ex-Con ($p<0.05$, respectively) (Fig. 5A–D).

miR-133b-Enriched Exosomes Downregulate the Protein Level of RABEPK

MVBs can either be routed to lysosomes for degradation or to exosomes for secretion[65]. Lysosomal dysfunction increases exosomal release[66,67]; RABEPK, cooperating with Rab9, participates in the endosome-to-trans-Golgi network (TGN) transport, which is essential for the lysosome formation[68]. Using Western blot and immunohistochemistry staining of IBZ tissues, we therefore examined whether the exosomal treatment affects RABEPK. Our data revealed that ischemia increased RABEPK protein levels, whereas the Ex-Con treatment significantly reduced MCAO-increased RABEPK proteins and the Ex-miR-133b$^+$ treatment further decreased the protein level ($p<0.05$, respectively) (Fig. 6A and B). Double immunofluorescence staining showed the RABEPK immunoreactivity was largely localized to GFAP$^+$ astrocytes (Fig. 6E–H). We then employed OGD astrocytes to further examine the effect of MSC exosomes on RABEPK expression in astrocytes. We found that the Ex-Con treatment significantly reduced RABEPK protein levels in the astrocytes subjected to OGD, and the Ex-miR-133b$^+$ treatment further lowered the protein level ($p<0.05$, respectively) (Fig. 6C and D).

DISCUSSION

Exosomes released by transplanted cells mediate the benefits of cell-based therapies for stroke[6,8,69,70]. It is therefore reasonable to consider replacing cell-based therapy for stroke with cell-free exosome-based treatment, which would minimize potential adverse effects of administering replicating and embolism-forming cells[71]. We therefore employed exosomes harvested from naive MSCs to treat experimental stroke models and found that the therapeutic effects of exosomes were consistent with the therapeutic effects of direct MSC treatment[7]. In the current study, we extended this exosome therapy concept to tailor the miRNA content of the exosomes. On the basis of studies indicating that miR-133b promotes neurovascular plasticity, we generated and employed exosomes enriched with miR-133b for the treatment of rats subjected to MCAO. We found that miR-133b-enriched exosomes significantly amplified the therapeutic benefits for stroke compared to control MSC exosomes. Our in vivo and in vitro studies also suggest that astrocytes and possibly other neural parenchymal cells participate in

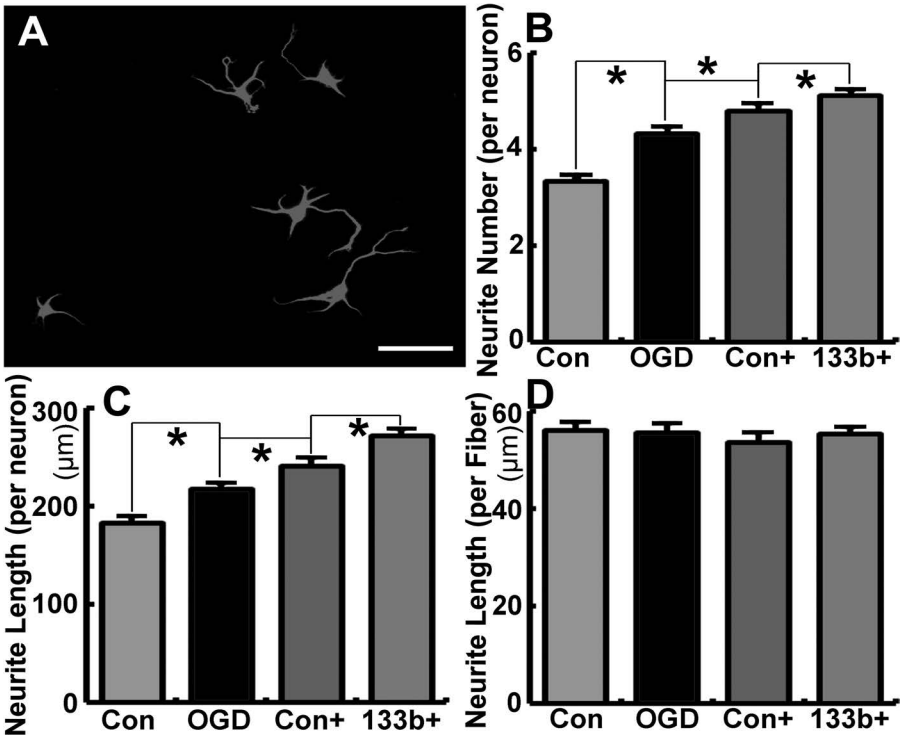

Figure 5. Exosomes harvested from oxygen- and glucose-deprived (OGD) astrocytes after treatment with miR-133b-overexpressing MSCs (Ex-miR-133b$^+$) increase neurite outgrowth. (A) The morphology of cultured neurons in this assay. Exosomes harvested from OGD astrocytes significantly increased the neurite number and total neurite length per neuron compared with the non-exosome-treated primary cultured cortical neurons. The neurite number and total neurite length substantially increased after the neurons were treated with exosomes harvested from OGD astrocytes that were pretreated by the MSCs infected with blank vector (Ex-Con) and Ex-miR-133b$^+$, and Ex-miR-133b$^+$-pretreated OGD astrocytic exosomes have the enhanced effect compared with the Ex-Con pretreatment ($p<0.05$, respectively; B–D). Con, non-exosome-treated neurons; OGD, neurons treated with exosomes harvested from OGD astrocytes; Con$^+$, neurons treated with exosomes harvested from OGD astrocytes pretreated with Ex-Con; 133b$^+$, neurons treated with exosomes harvested from OGD astrocytes pretreated with Ex-miR-133b$^+$. *$p<0.05$, mean ± standard deviation (SD), $n=3$/group. Scale bar: 50 μm.

the enhanced functional recovery for stroke induced by miR-133b-enriched exosomes. miR-133b increased the secondary release of exosomes from astrocytes, which appear to more potently enhance neurite outgrowth and plasticity than naive MSC exosomes. Thus, our study provides the basis for engineering miRNA content of exosomes that concurrently regulate multiple molecular pathways and further promote restorative processes, and that exosomes, whether naive or engineered, induce secondary release of astrocytic exosomes. Here we focused on astrocytes, and we do not exclude the possibility that other parenchymal and inflammatory or vascular cells may also release secondary exosomes in response to primary exosome stimulation.

EVs, including exosomes, are involved in intercellular communication within the nervous system[54] and play major roles in neurological diseases and in nerve trauma[72,73], as well as mediate signaling during brain development and function[74]. Exosomes released by brain parenchymal cells modulate neuron–glial–vascular communication and support neural plasticity[33,56,57,75,76]. By modulating the interactions between glia and neurons, glial-derived exosomes promote neurite outgrowth and neuronal survival under high neuronal activity and/or oxidative stress condition[33]. miR-133b-enriched exosomes increased exosome content within the IBZ. This increase may be attributed to exosomes generated by astrocytes. However, as noted, we cannot exclude the possibility that the preferential increase of exosomes released by other neural parenchymal cells induced by miR-133b-enriched exosomes may also participate in the enhanced neural plasticity and functional recovery, since other brain parenchymal cells (e.g., oligodendrocytes) also secrete exosomes that contain major myelin- and stress-protective proteins, and these exosomes are involved in glia-mediated trophic support to axons[16].

MVBs are generated by inward budding of the late endosomal membrane, which gives rise to intraluminal

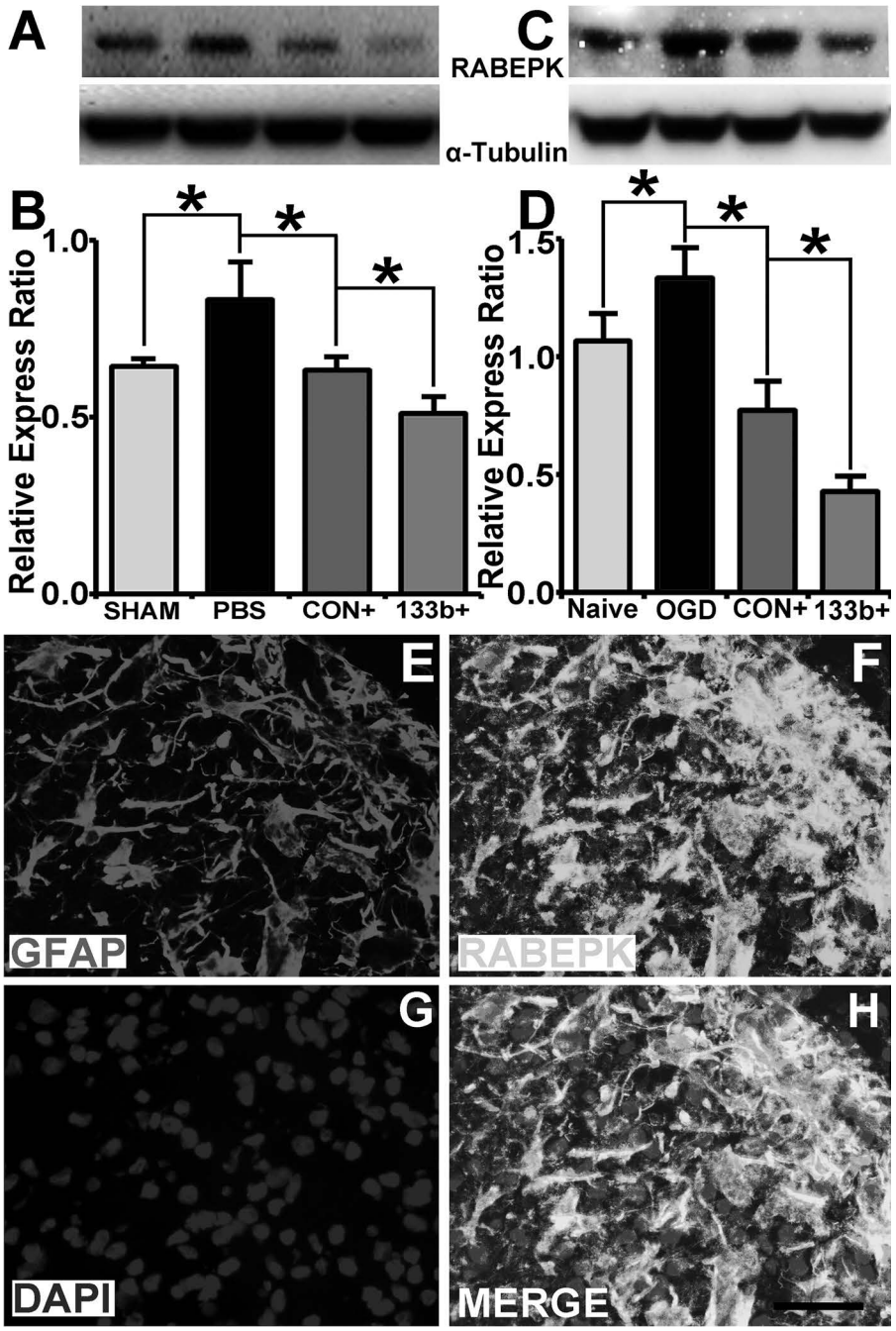

Figure 6. MicroRNA 133b (miR-133b)-enriched exosomes downregulate the protein level of Rab9 effector protein with kelch motifs (RABEPK). Western blot data show that the MSCs infected with blank vector (Ex-Con) treatment significantly downregulated the RABEPK level increased in the ischemic boundary zone (IBZ) after middle cerebral artery occlusion (MCAO), and miR-133b-over-expressing MSC (Ex-miR-133b$^+$) treatment further reduces the protein level (A, B) ($p<0.05$, respectively). Double immunostaining shows the RABEPK largely expressed in the astrocytes (E–H). Ex-Con treatment significantly reduced the RABEPK level increase in the astrocytes subjected to oxygen and glucose deprivation (OGD), and Ex-miR-133b$^+$ treatment further reduces the protein level (C, D) ($p<0.05$, respectively). Sham, tissue from sham surgery rats; PBS, MCAO rats treated with phosphate-buffered saline (PBS); Naive, naive astrocytes; OGD, astrocytes subjected to OGD; CON$^+$, MCAO rats or OGD astrocytes treated with Ex-Con; 133b$^+$, MCAO rats or OGD astrocytes treated with Ex-miR-133b$^+$. *$p<0.05$, mean ± standard deviation (SD), $n=3$/group. Scale bar: 50 μm.

vesicles (ILVs) within late endosomes[65]. MVBs can be either routed to lysosomes for degradation or fused with the plasma membrane to discharge their ILVs as exosomes to the extracellular space. Delivery of lysosomal enzymes is essential for the maintenance of proper functioning lysosomes, which include addition of a specific lysosomal tag, mannose 6-phosphate (M6P), to peptides, for example, lysosomal hydrolases. With binding of these tags to M6P receptors in the Golgi apparatus and proper packaging into vesicles destined for the lysosomal system, the hydrolases are released in the acidic environment of endosomes, and the receptor is retrieved to the Golgi by retromer and Rab9[77,78]. RABEPK is required for this endosome-to-TGN transport[68], so the lack of RABEPK may lead to reduced lysosome formation. Lysosomal dysfunction causes increased exosomal release[66,67,79,80]. Our data suggest that increased RABEPK level in the IBZ may consequently increase the lysosome formation. These data are consistent with prior studies showing that the autophagy and lysosomal degradation pathways are stimulated in hypoxia–ischemia-induced brain injury[81–85]. Endocytosis and autophagy cooperate and share molecular machinery, such as the Rab GTPase network[86–89]. The structure of the autophagy pathway, the autophagosome, can fuse with endocytic structures such as MVBs to generate the amphisome, which fuses with the lysosome to degrade the material wrapped inside[90–93]. Hypoxia induces exosome release as well[13,94]. Impacting the balance between the autophagy and lysosome pathways, by inhibiting the lysosome formation, may increase the exosome release. The RABEPK expression was downregulated after miR-133b-enriched exosome treatment in the IBZ may effect on increasing exosomal release from astrocytes. RABEPK is one of the putative genes targeted by miR-206 (Targetscan.org), while transforming growth factor-β (TGF-β) inhibits miR-206 levels[95]. Although it does not directly target the RABEPK gene, miR-133b negatively regulates the TGF-β signal pathway activity[96], which may lead to the decrease of RABEPK expression. Thus, further investigations on the regulation of miR-133b on miR-206 expression and subsequently on RABEPK protein level, as well as the balance of lysosome formation and exosome generation, are warranted.

Exosomes penetrate the brain–blood barrier (BBB)[97,98]; however, the detailed mechanisms are unclear. Transcytosis in epithelial cells may participate in the process[99,100]. Transcytosis allows some materials to enter one side of a cell and exit from the opposite side. Possibly, in some circumstances, exosomes in the vessel lumen side may be endocytosed by the endothelial cell of the BBB to form as late endosomes/MVBs and then fuse with the plasma membrane instead of with lysosomes, releasing the engulfed exosomes, into the brain parenchymal side extracellular space. We administer the exosomes using an IA approach in the current study to reduce potential liver and lung sequestration. Interestingly, our previous study, which employed IV administration of naive MSC exosomes[7], also showed beneficial effects on the stroke restoration, may suggest that in addition to directly affecting brain parenchymal cells, administration of exosomes may also have systemic effects that participate their restorative effects after stroke. Given that miR-133b-enriched exosomes increase the secondary release of exosomes from astrocytes, they may also interact with endothelial cells and increase the exosomes released by endothelial cells.

There are a number of caveats to consider. We have previously demonstrated that treatment of stroke with downregulated miR-133b in MSCs significantly reduces functional recovery after MCAO compared with naive MSC-treated animals, and treatment with MSCs enriched in miR-133b significantly enhances functional recovery compared with naive MSC-treated animals[6]. Importantly, our data indicated that the therapeutic effects were mediated by exosome transfer of miR-133b from the MSCs to the brain. In the present study, our primary goal was to demonstrate, as a proof of principle, that we can further improve functional recovery by administering tailored exosomes enriched in miR-133b. Further studies, in which miR-133b exosome content is reduced to verify the function of exosomal miR-133b, are warranted. Although volumes of cerebral infarction are not altered by the MSCs and MSC exosome treatment[2,7], we cannot exclude the possibility that treatment with exosomes harvested from miR-133b-overexpressing MSCs at 24 h poststroke also evokes some neuroprotective benefits in the ischemic boundary region.

CONCLUSIONS

IA-administered exosomes harvested from miR-133b-overexpressing MSCs improve neural plasticity and functional recovery after stroke beyond that of naive exosomes. Exosomes enriched with mature miR-133b from miR-133b-overexpressing MSCs further stimulate and increase exosomes release from astrocytes, possibly by downregulating the RABEPK expression. The exosomes derived from OGD astrocytes pretreated with miR-133b-enriched exosomes promote neurite outgrowth and elongation in vitro. We thus propose that the contribution of the secondary astrocytic exosome release may contribute to brain plasticity and subsequent neurological recovery after stroke.

ACKNOWLEDGMENTS: Research reported in this publication was supported by the National Institute of Neurological Disorders and Stroke (NINDS) of the National Institutes of Health under Award Nos. RO1 NS081189 (H.X.), RO1 NS075156 (Z.G.Z.), and RO1 NS088656 (M.C.). The content is solely the responsibility of the authors and does not necessarily represent the official views of the National Institutes of Health. The authors thank Cindi Roberts, Julie Landschoot-Ward, and Sue

Santra for technical assistance on histology, and Amy Kemper for technical assistance on TEM. Author contributions: Hongqi Xin—conception and design, collection and/or assembly of data, data analysis and interpretation, financial support, and manuscript writing; Fengjie Wang—collection and/or assembly of data; Yanfeng Li—collection and/or assembly of data; Qing-e Lu—collection and/or assembly of data; Wing Lee Cheung—collection and/or assembly of data; Yi Zhang—collection and/or assembly of data; Zheng Gang Zhang—conception and design, data analysis and interpretation, and manuscript writing; Michael Chopp—conception and design, data analysis and interpretation, financial support, manuscript writing, and final approval of the manuscript. The authors declare no conflicts of interest.

REFERENCES

1. Chen J, Li Y, Wang L, Lu M, Zhang X, Chopp M. Therapeutic benefit of intracerebral transplantation of bone marrow stromal cells after cerebral ischemia in rats. J Neurol Sci. 2001;189(1–2):49–57.
2. Chen J, Li Y, Wang L, Zhang Z, Lu D, Lu M, Chopp M. Therapeutic benefit of intravenous administration of bone marrow stromal cells after cerebral ischemia in rats. Stroke 2001;32(4):1005–11.
3. Andrews EM, Tsai SY, Johnson SC, Farrer JR, Wagner JP, Kopen GC, Kartje GL. Human adult bone marrow-derived somatic cell therapy results in functional recovery and axonal plasticity following stroke in the rat. Exp Neurol. 2008;211(2):588–92.
4. Chopp M, Li Y. Treatment of stroke and intracerebral hemorrhage with cellular and pharmacological restorative therapies. Acta Neurochir Suppl. 2008;105:79–83.
5. Chopp M, Li Y, Zhang J. Plasticity and remodeling of brain. J Neurol Sci. 2008;265(1–2):97–101.
6. Xin H, Li Y, Liu Z, Wang X, Shang X, Cui Y, Zhang ZG, Chopp M. MiR-133b promotes neural plasticity and functional recovery after treatment of stroke with multipotent mesenchymal stromal cells in rats via transfer of exosome-enriched extracellular particles. Stem Cells 2013;31(12):2737–46.
7. Xin H, Li Y, Cui Y, Yang JJ, Zhang ZG, Chopp M. Systemic administration of exosomes released from mesenchymal stromal cells promote functional recovery and neurovascular plasticity after stroke in rats. J Cereb Blood Flow Metab. 2013;33(11):1711–5.
8. Xin H, Li Y, Buller B, Katakowski M, Zhang Y, Wang X, Shang X, Zhang ZG, Chopp M. Exosome-mediated transfer of miR-133b from multipotent mesenchymal stromal cells to neural cells contributes to neurite outgrowth. Stem Cells 2012;30(7):1556–64.
9. Zhang Y, Chopp M, Zhang ZG, Katakowski M, Xin H, Qu C, Ali M, Mahmood A, Xiong Y. Systemic administration of cell-free exosomes generated by human bone marrow derived mesenchymal stem cells cultured under 2D and 3D conditions improves functional recovery in rats after traumatic brain injury. Neurochem Int. 2016.
10. Zhang Y, Chopp M, Meng Y, Katakowski M, Xin H, Mahmood A, Xiong Y. Effect of exosomes derived from multipluripotent mesenchymal stromal cells on functional recovery and neurovascular plasticity in rats after traumatic brain injury. J Neurosurg. 2015;122(4):856–67.
11. Fruhbeis C, Helmig S, Tug S, Simon P, Kramer-Albers EM. Physical exercise induces rapid release of small extracellular vesicles into the circulation. J Extracell Vesicles 2015;4:28239.
12. Kucharzewska P, Belting M. Emerging roles of extracellular vesicles in the adaptive response of tumour cells to microenvironmental stress. J Extracell Vesicles 2013;2.
13. King HW, Michael MZ, Gleadle JM. Hypoxic enhancement of exosome release by breast cancer cells. BMC Cancer 2012;12(1):421.
14. Savina A, Furlan M, Vidal M, Colombo MI. Exosome release is regulated by a calcium-dependent mechanism in K562 cells. J Biol Chem. 2003;278(22):20083–90.
15. Faure J, Lachenal G, Court M, Hirrlinger J, Chatellard-Causse C, Blot B, Grange J, Schoehn G, Goldberg Y, Boyer V and others. Exosomes are released by cultured cortical neurones. Mol Cell Neurosci. 2006;31(4):642–8.
16. Kramer-Albers EM, Bretz N, Tenzer S, Winterstein C, Mobius W, Berger H, Nave KA, Schild H, Trotter J. Oligodendrocytes secrete exosomes containing major myelin and stress-protective proteins: Trophic support for axons? Proteomics Clin Appl. 2007;1(11):1446–61.
17. Lachenal G, Pernet-Gallay K, Chivet M, Hemming FJ, Belly A, Bodon G, Blot B, Haase G, Goldberg Y, Sadoul R. Release of exosomes from differentiated neurons and its regulation by synaptic glutamatergic activity. Mol Cell Neurosci. 2011;46(2):409–18.
18. Riches A, Campbell E, Borger E, Powis S. Regulation of exosome release from mammary epithelial and breast cancer cells—A new regulatory pathway. Eur J Cancer 2014;50(5):1025–34.
19. Pols MS, Klumperman J. Trafficking and function of the tetraspanin CD63. Exp Cell Res. 2009;315(9):1584–92.
20. Suetsugu A, Honma K, Saji S, Moriwaki H, Ochiya T, Hoffman RM. Imaging exosome transfer from breast cancer cells to stroma at metastatic sites in orthotopic nude-mouse models. Adv Drug Deliv Rev. 2013;65(3):383–90.
21. Hazawa M, Tomiyama K, Saotome-Nakamura A, Obara C, Yasuda T, Gotoh T, Tanaka I, Yakumaru H, Ishihara H, Tajima K. Radiation increases the cellular uptake of exosomes through CD29/CD81 complex formation. Biochem Biophys Res Commun. 2014;446(4):1165–71.
22. Abache T, Le Naour F, Planchon S, Harper F, Boucheix C, Rubinstein E. The transferrin receptor and the tetraspanin web molecules CD9, CD81, and CD9P-1 are differentially sorted into exosomes after TPA treatment of K562 cells. J Cell Biochem. 2007;102(3):650–64.
23. Baddoo M, Hill K, Wilkinson R, Gaupp D, Hughes C, Kopen GC, Phinney DG. Characterization of mesenchymal stem cells isolated from murine bone marrow by negative selection. J Cell Biochem. 2003;89(6):1235–49.
24. Meirelles Lda S, Nardi NB. Murine marrow-derived mesenchymal stem cell: Isolation, in vitro expansion, and characterization. Br J Haematol. 2003;123(4):702–11.
25. Tropel P, Noel D, Platet N, Legrand P, Benabid AL, Berger F. Isolation and characterisation of mesenchymal stem cells from adult mouse bone marrow. Exp Cell Res. 2004;295(2):395–406.
26. Choi H, Lee DS. Illuminating the physiology of extracellular vesicles. Stem Cell Res Ther. 2016;7(1):55.
27. Bala S, Csak T, Momen-Heravi F, Lippai D, Kodys K, Catalano D, Satishchandran A, Ambros V, Szabo G. Biodistribution and function of extracellular miRNA-155 in mice. Sci Rep. 2015;5:10721.

28. Li Y, Powers C, Jiang N, Chopp M. Intact, injured, necrotic and apoptotic cells after focal cerebral ischemia in the rat. J Neurol Sci. 1998;156(2):119–32.
29. Chen J, Zhang ZG, Li Y, Wang L, Xu YX, Gautam SC, Lu M, Zhu Z, Chopp M. Intravenous administration of human bone marrow stromal cells induces angiogenesis in the ischemic boundary zone after stroke in rats. Circ Res. 2003;92(6):692–9.
30. Chen H, Chopp M, Zhang ZG, Garcia JH. The effect of hypothermia on transient middle cerebral artery occlusion in the rat. J Cereb Blood Flow Metab. 1992;12(4): 621–8.
31. Stroemer RP, Kent TA, Hulsebosch CE. Neocortical neural sprouting, synaptogenesis, and behavioral recovery after neocortical infarction in rats. Stroke 1995; 26(11):2135–44.
32. Li Y, Chen J, Chopp M. Adult bone marrow transplantation after stroke in adult rats. Cell Transplant. 2001; 10(1):31–40.
33. Wang S, Cesca F, Loers G, Schweizer M, Buck F, Benfenati F, Schachner M, Kleene R. Synapsin I is an oligomannose-carrying glycoprotein, acts as an oligomannose-binding lectin, and promotes neurite outgrowth and neuronal survival when released via glia-derived exosomes. J Neurosci. 2011;31(20):7275–90.
34. Perez-Gonzalez R, Gauthier SA, Kumar A, Levy E. The exosome secretory pathway transports amyloid precursor protein carboxyl-terminal fragments from the cell into the brain extracellular space. J Biol Chem. 2012;287(51):43108–15.
35. Orozco AF, Lewis DE. Flow cytometric analysis of circulating microparticles in plasma. Cytometry A 2010; 77(6):502–14.
36. Liu X, Wang HW. Single particle electron microscopy reconstruction of the exosome complex using the random conical tilt method. J Vis Exp. 2011(49).
37. Bhatnagar S, Schorey JS. Exosomes released from infected macrophages contain Mycobacterium avium glycopeptidolipids and are proinflammatory. J Biol Chem. 2007;282(35):25779–89.
38. Xin H, Li Y, Shen LH, Liu X, Hozeska-Solgot A, Zhang RL, Zhang ZG, Chopp M. Multipotent mesenchymal stromal cells increase tPA expression and concomitantly decrease PAI-1 expression in astrocytes through the sonic hedgehog signaling pathway after stroke (in vitro study). J Cereb Blood Flow Metab. 2011;31(11):2181–8.
39. Xin H, Li Y, Shen LH, Liu X, Wang X, Zhang J, Pourabdollah-Nejad DS, Zhang C, Zhang L, Jiang H, and others. Increasing tPA activity in astrocytes induced by multipotent mesenchymal stromal cells facilitate neurite outgrowth after stroke in the mouse. PLoS One 2010; 5(2):e9027.
40. Wang L, Zhang ZG, Zhang RL, Jiao ZX, Wang Y, Pourabdollah-Nejad DS, LeTourneau Y, Gregg SR, Chopp M. Neurogenin 1 mediates erythropoietin enhanced differentiation of adult neural progenitor cells. J Cereb Blood Flow Metab. 2006;26(4):556–64.
41. Stanely C BM. A method for intra-vital staining with silver ammonium oxide solution. J Psychol Neurol. 1925;31:4.
42. Kluver H, Barrera E. A method for the combined staining of cells and fibers in the nervous system. J Neuropathol Exp Neurol. 1953;12(4):400–3.
43. Grady MS, McLaughlin MR, Christman CW, Valadka AB, Fligner CL, Povlishock JT. The use of antibodies targeted against the neurofilament subunits for the detection of diffuse axonal injury in humans. J Neuropathol Exp Neurol. 1993;52(2):143–52.
44. Calhoun ME, Jucker M, Martin LJ, Thinakaran G, Price DL, Mouton PR. Comparative evaluation of synaptophysin-based methods for quantification of synapses. J Neurocytol. 1996;25(12):821–8.
45. Li Y, Sharov VG, Jiang N, Zaloga C, Sabbah HN, Chopp M. Ultrastructural and light microscopic evidence of apoptosis after middle cerebral artery occlusion in the rat. Am J Pathol. 1995;146(5):1045–51.
46. Seyfried DM, Han Y, Yang D, Ding J, Chopp M. Erythropoietin promotes neurological recovery after intracerebral haemorrhage in rats. Int J Stroke 2009; 4(4):250–6.
47. Lu M, Chen J, Lu D, Yi L, Mahmood A, Chopp M. Global test statistics for treatment effect of stroke and traumatic brain injury in rats with administration of bone marrow stromal cells. J Neurosci Methods 2003; 128(1–2):183–90.
48. Julie M. LEGLER ML, and Louise M. RYAN. Efficiency and power of tests for multiple binary outcomes. Journal of the American Statistical Association 1995;90(430):14.
49. Stys PK. Anoxic and ischemic injury of myelinated axons in CNS white matter: From mechanistic concepts to therapeutics. J Cereb Blood Flow Metab. 1998;18(1):2–25.
50. Pant HC, Veeranna. Neurofilament phosphorylation. Biochem Cell Biol. 1995;73(9–10):575–92.
51. Sceneay J, Smyth MJ, Moller A. The pre-metastatic niche: Finding common ground. Cancer Metastasis Rev. 2013;32(3–4):449–64.
52. Ujike H, Takaki M, Kodama M, Kuroda S. Gene expression related to synaptogenesis, neuritogenesis, and MAP kinase in behavioral sensitization to psychostimulants. Ann N Y Acad Sci. 2002;965:55–67.
53. Chivet M, Hemming F, Pernet-Gallay K, Fraboulet S, Sadoul R. Emerging role of neuronal exosomes in the central nervous system. Front Physiol. 2012;3:145.
54. Rajendran L, Bali J, Barr MM, Court FA, Kramer-Albers EM, Picou F, Raposo G, van der Vos KE, van Niel G, Wang J and others. Emerging roles of extracellular vesicles in the nervous system. J Neurosci. 2014;34(46):15482–9.
55. Fruhbeis C, Frohlich D, Kramer-Albers EM. Emerging roles of exosomes in neuron-glia communication. Front Physiol. 2012;3:119.
56. Wang G, Dinkins M, He Q, Zhu G, Poirier C, Campbell A, Mayer-Proschel M, Bieberich E. Astrocytes secrete exosomes enriched with proapoptotic ceramide and prostate apoptosis response 4 (PAR-4): Potential mechanism of apoptosis induction in Alzheimer disease (AD). J Biol Chem. 2012;287(25):21384–95.
57. Fruhbeis C, Frohlich D, Kuo WP, Kramer-Albers EM. Extracellular vesicles as mediators of neuron-glia communication. Front Cell Neurosci. 2013;7:182.
58. Zhang ZG, Chopp M. Exosomes in stroke pathogenesis and therapy. J Clin Invest. 2016;126(4):1190–7.
59. Pekny M, Pekna M. Astrocyte reactivity and reactive astrogliosis: Costs and benefits. Physiol Rev. 2014;94(4): 1077–98.
60. Li Y, Liu Z, Xin H, Chopp M. The role of astrocytes in mediating exogenous cell-based restorative therapy for stroke. Glia 2014;62(1):1–16.
61. Sen E, Levison SW. Astrocytes and developmental white matter disorders. Ment Retard Dev Disabil Res Rev. 2006; 12(2):97–104.

62. Dugan LL, Kim-Han JS. Astrocyte mitochondria in in vitro models of ischemia. J Bioenerg Biomembr. 2004;36(4):317–21.
63. Gao Q, Li Y, Shen L, Zhang J, Zheng X, Qu R, Liu Z, Chopp M. Bone marrow stromal cells reduce ischemia-induced astrocytic activation in vitro. Neuroscience 2008; 152(3):646–55.
64. Shen LH, Li Y, Chopp M. Astrocytic endogenous glial cell derived neurotrophic factor production is enhanced by bone marrow stromal cell transplantation in the ischemic boundary zone after stroke in adult rats. Glia 2010;58(9): 1074–81.
65. Keller S, Sanderson MP, Stoeck A, Altevogt P. Exosomes: From biogenesis and secretion to biological function. Immunol Lett. 2006;107(2):102–8.
66. Alvarez-Erviti L, Seow Y, Schapira AH, Gardiner C, Sargent IL, Wood MJ, Cooper JM. Lysosomal dysfunction increases exosome-mediated alpha-synuclein release and transmission. Neurobiol Dis. 2011;42(3):360–7.
67. Mohamed NV, Plouffe V, Remillard-Labrosse G, Planel E, Leclerc N. Starvation and inhibition of lysosomal function increased tau secretion by primary cortical neurons. Sci Rep. 2014;4:5715.
68. Diaz E, Schimmoller F, Pfeffer SR. A novel Rab9 effector required for endosome-to-TGN transport. J Cell Biol. 1997;138(2):283–90.
69. Hu G, Drescher KM, Chen XM. Exosomal miRNAs: Biological properties and therapeutic potential. Front Genet. 2012;3:56.
70. Doeppner TR, Herz J, Gorgens A, Schlechter J, Ludwig AK, Radtke S, de Miroschedji K, Horn PA, Giebel B, Hermann DM. Extracellular vesicles improve post-stroke neuroregeneration and prevent postischemic immunosuppression. Stem Cells Transl Med. 2015;4(10):1131–43.
71. Wang Y, Han ZB, Song YP, Han ZC. Safety of mesenchymal stem cells for clinical application. Stem Cells Int. 2012;2012:652034.
72. Von Bartheld CS, Altick AL. Multivesicular bodies in neurons: Distribution, protein content, and trafficking functions. Prog Neurobiol. 2011;93(3):313–40.
73. Wood MJ, O'Loughlin AJ, Samira L. Exosomes and the blood-brain barrier: Implications for neurological diseases. Ther Deliv. 2011;2(9):1095–9.
74. Sharma P, Schiapparelli L, Cline HT. Exosomes function in cell-cell communication during brain circuit development. Curr Opin Neurobiol. 2013;23(6):997–1004.
75. Gosselin RD, Meylan P, Decosterd I. Extracellular microvesicles from astrocytes contain functional glutamate transporters: Regulation by protein kinase C and cell activation. Front Cell Neurosci. 2013;7:251.
76. Lopez-Verrilli MA, Picou F, Court FA. Schwann cell-derived exosomes enhance axonal regeneration in the peripheral nervous system. Glia 2013;61(11):1795–806.
77. Arighi CN, Hartnell LM, Aguilar RC, Haft CR, Bonifacino JS. Role of the mammalian retromer in sorting of the cation-independent mannose 6-phosphate receptor. J Cell Biol. 2004;165(1):123–33.
78. Riederer MA, Soldati T, Shapiro AD, Lin J, Pfeffer SR. Lysosome biogenesis requires Rab9 function and receptor recycling from endosomes to the trans-Golgi network. J Cell Biol. 1994;125(3):573–82.
79. Goetzl EJ, Boxer A, Schwartz JB, Abner EL, Petersen RC, Miller BL, Kapogiannis D. Altered lysosomal proteins in neural-derived plasma exosomes in preclinical Alzheimer disease. Neurology 2015;85(1):40–7.
80. Emmanouilidou E, Vekrellis K. Exocytosis and spreading of normal and aberrant alpha-synuclein. Brain Pathol. 2016; 26(3):398–403.
81. Lipton P. Lysosomal membrane permeabilization as a key player in brain ischemic cell death: A "lysosomocentric" hypothesis for ischemic brain damage. Transl Stroke Res. 2013;4(6):672–84.
82. Han F, Chen YX, Lu YM, Huang JY, Zhang GS, Tao RR, Ji YL, Liao MH, Fukunaga K, Qin ZH. Regulation of the ischemia-induced autophagy-lysosome processes by nitrosative stress in endothelial cells. J Pineal Res. 2011;51(1):124–35.
83. Gu Z, Sun Y, Liu K, Wang F, Zhang T, Li Q, Shen L, Zhou L, Dong L, Shi N and others. The role of autophagic and lysosomal pathways in ischemic brain injury. Neural Regen Res. 2013;8(23):2117–25.
84. Balduini W, Carloni S, Buonocore G. Autophagy in hypoxia-ischemia induced brain injury: Evidence and speculations. Autophagy 2009;5(2):221–3.
85. Galluzzi L, Bravo-San Pedro JM, Blomgren K, Kroemer G. Autophagy in acute brain injury. Nat Rev Neurosci. 2016;17(8):467–84.
86. Tooze SA, Abada A, Elazar Z. Endocytosis and autophagy: Exploitation or cooperation? Cold Spring Harb Perspect Biol. 2014;6(5):a018358.
87. Ao X, Zou L, Wu Y. Regulation of autophagy by the Rab GTPase network. Cell Death Differ. 2014;21(3): 348–58.
88. Hyttinen JM, Niittykoski M, Salminen A, Kaarniranta K. Maturation of autophagosomes and endosomes: A key role for Rab7. Biochim Biophys Acta 2013; 1833(3):503–10.
89. Lamb CA, Dooley HC, Tooze SA. Endocytosis and autophagy: Shared machinery for degradation. Bioessays 2013;35(1):34–45.
90. Fader CM, Colombo MI. Autophagy and multivesicular bodies: Two closely related partners. Cell Death Differ. 2009;16(1):70–8.
91. Filimonenko M, Stuffers S, Raiborg C, Yamamoto A, Malerod L, Fisher EM, Isaacs A, Brech A, Stenmark H, Simonsen A. Functional multivesicular bodies are required for autophagic clearance of protein aggregates associated with neurodegenerative disease. J Cell Biol. 2007;179(3):485–500.
92. Rusten TE, Simonsen A. ESCRT functions in autophagy and associated disease. Cell Cycle 2008;7(9):1166–72.
93. Muller M, Schmidt O, Angelova M, Faserl K, Weys S, Kremser L, Pfaffenwimmer T, Dalik T, Kraft C, Trajanoski Z and others. The coordinated action of the MVB pathway and autophagy ensures cell survival during starvation. Elife 2015;4:e07736.
94. Kucharzewska P, Christianson HC, Welch JE, Svensson KJ, Fredlund E, Ringner M, Morgelin M, Bourseau-Guilmain E, Bengzon J, Belting M. Exosomes reflect the hypoxic status of glioma cells and mediate hypoxia-dependent activation of vascular cells during tumor development. Proc Natl Acad Sci USA 2013.
95. Winbanks CE, Wang B, Beyer C, Koh P, White L, Kantharidis P, Gregorevic P. TGF-beta regulates miR-206 and miR-29 to control myogenic differentiation through regulation of HDAC4. J Biol Chem. 2011;286(16):13805–14.

96. Robinson PM, Chuang TD, Sriram S, Pi L, Luo XP, Petersen BE, Schultz GS. MicroRNA signature in wound healing following excimer laser ablation: Role of miR-133b on TGFbeta1, CTGF, SMA, and COL1A1 expression levels in rabbit corneal fibroblasts. Invest Ophthalmol Vis Sci. 2013;54(10):6944–51.
97. Alvarez-Erviti L, Seow Y, Yin H, Betts C, Lakhal S, Wood MJ. Delivery of siRNA to the mouse brain by systemic injection of targeted exosomes. Nat Biotechnol. 2011;29(4):341–5.
98. Yang T, Martin P, Fogarty B, Brown A, Schurman K, Phipps R, Yin VP, Lockman P, Bai S. Exosome delivered anticancer drugs across the blood-brain barrier for brain cancer therapy in Danio rerio. Pharm Res. 2015;32(6):2003–14.
99. Dohgu S, Banks WA. Brain pericytes increase the lipopolysaccharide-enhanced transcytosis of HIV-1 free virus across the in vitro blood-brain barrier: Evidence for cytokine-mediated pericyte-endothelial cell crosstalk. Fluids Barriers CNS 2013;10(1):23.
100. Tuma P, Hubbard AL. Transcytosis: Crossing cellular barriers. Physiol Rev. 2003;83(3):871–932.